Conformational Changes within the Cytosolic Portion of Phospholamban upon Release of Ca-ATPase Inhibition†

Jinhui Li, Diana J. Bigelow, and Thomas C. Squier*

Cell Biology Group, Biological Sciences Division, Fundamental Sciences Directorate, Pacific Northwest National Laboratory, Richland, Washington 99352

Received December 4, 2003; Revised Manuscript Received January 19, 2004

ABSTRACT: Phospholamban (PLB) is a major target of the β-adrenergic cascade in the heart, functioning to modulate contractile force by altering the rate of calcium re-sequestration by the Ca-ATPase. Functionally, inhibition by PLB binding is manifested by shifts in the calcium dependence of Ca-ATPase activation toward higher calcium levels; phosphorylation of PLB by PKA reverses the inhibitory action of PLB. To investigate structural changes in the cytoplasmic portion of PLB that result from either the phosphorylation of PLB by cAMP-dependent protein kinase (PKA) or calcium binding to the Ca-ATPase, we have used frequency-domain fluorescence spectroscopy to measure the spatial separation and conformational heterogeneity between N-(1-pyrenyl)maleimide, covalently bound to a single cysteine (Cys^{24}) engineered near the membrane surface of the transmembrane domain of PLB, and Tyr^{6} in the cytosolic domain. Irrespective of calcium activation of the Ca-ATPase or phosphorylation of Ser^{16} in PLB by PKA, we find that PLB remains tightly associated with the Ca-ATPase in a well-defined conformation. However, calcium activation of the Ca-ATPase induces an increase in the overall dimensions of the cytoplasmic portion of bound PLB, whereas PLB phosphorylation results in a more compact structure, consistent with increased helical content induced by a salt link between phospho-Ser^{16} and Arg^{13}. Thus, enzyme activation of the Ca-ATPase may occur through different mechanisms: calcium binding to high-affinity sites within the Ca-ATPase functions to overcome conformational constraints imposed by PLB on the N-domain of the Ca-ATPase; alternatively, phosphorylation stabilizes the backbone fold of PLB to release inhibitory interactions with the Ca-ATPase.

Phospholamban (PLB)[1] is coexpressed with the Ca-ATPase in cardiac and slow-twitch skeletal muscle, and functions to shift the calcium dependence of Ca-ATPase activation toward higher calcium levels (*1*, *2*). This inhibitory action modulates the rate of calcium re-sequestration into the sarcoplasmic reticulum (SR) by the Ca-ATPase following excitation-contraction coupling, and in the heart it diminishes the strength of contraction (*3*−*7*). Following β-adrenergic stimulation, PLB is selectively phosphorylated at Ser^{16} by cAMP-dependent protein kinase (PKA), releasing the inhibitory interaction between PLB and the Ca-ATPase to accelerate rates of muscle relaxation and facilitate greater cardiac force generation.

The structural interaction between PLB and the Ca-ATPase responsible for enzyme inhibition involves both the transmembrane and cytosolic domains of PLB and the Ca-ATPase (*8*). Specific contact interactions have been identified through the use of cross-linking and mutagenesis measurements that suggest a proximal relationship between K^{3} near the amino-terminus of PLB and the $KDDKPVK^{403}$ binding sequence within the nucleotide-binding domain of the Ca-ATPase, while maintaining contact interactions between the transmembrane domain of PLB (i.e., N^{27}, N^{30}, and V^{49}) and sites on transmembrane helix M4 of the Ca-ATPase (i.e., L^{321}, C^{318}, and V^{89}) (*9*−*11*). Structural measurements of PLB bound to the Ca-ATPase indicate a requirement for reorientation of the nucleotide-binding domain of the Ca-ATPase, bringing it into closer proximity with the membrane surface to accommodate its complexation with PLB (*12*). This requirement is consistent with prior measurements demonstrating that phosphorylation of PLB by PKA results in a 10° angular reorientation of the nucleotide-binding domain of the Ca-ATPase (*5*, *13*). Thus, conformational constraints imposed on domain movements of the Ca-ATPase appear to underlie the functional regulation of transport activity by PLB.

Alterations in the structure of the hinge element connecting the cytosolic (residues 4−16) and transmembrane (residues 22−49) helical domains of PLB following phosphorylation of PLB by PKA have been suggested to underlie the

† This work was supported by a grant from the National Institutes of Health (HL64031).

* Corresponding author. Address: Pacific Northwest National Laboratory, P.O. Box 999, Mail Stop P7-53; Richland, WA 99352. E-mail: thomas.squier@pnl.gov. Tel: (509) 376-2218. Fax: (509) 376-1494.

[1] Abbreviations: ATP, adenosine 5′-triphosphate; cAMP, adenosine 3′:5′-cyclic monophosphate; CCCP, carbonyl cyanide 3-chlorophenyhydrazone; $C_{12}E_9$, polyoxyethylene 9 lauryl ether; EGTA, ethylene glycol-bis(β-aminoethyl ether)-N,N,N′,N′-tetraacetic acid; MOPS, 3-(N-morpholino)propane-sulfonic acid; OG, *n*-octyl β-d-glucopyranoside; PKA, cAMP-dependent protein kinase; PLB, phospholamban; PMal, N−(1-pyrenyl) maleimide; POPOP, 1,4-bis [5-phenyl-2-oxazolyl]-benzene; SDS, sodium dodecyl sulfate; SDS−PAGE, sodium dodecyl sulfate−polyacrylamide gel electrophoresis; SERCA, sarco(endo)-plasmic Ca-ATPase; SR, sarcoplasmic reticulum; TNM, tetranitromethane.

10.1021/bi036183u CCC: $27.50
Published on Web 03/09/2004

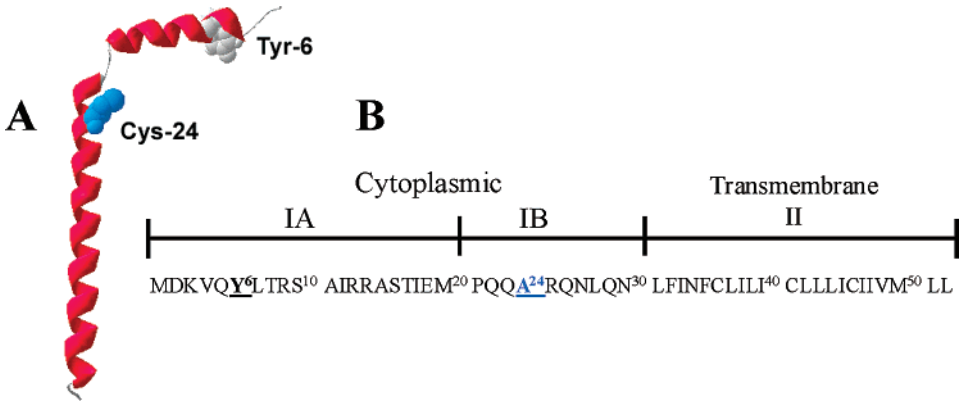

FIGURE 1: Depiction of backbone fold of PLB (A) (1FJK; *40*) and suggested domain structure (B). Relative positions of donor chromophore PMal (blue) covalently bound to position A24C and acceptor chromophore nitrotyrosine (grey) at position 6 are highlighted. The complete amino acid sequence of cytoplasmic (IA and IB) and transmembrane domains of PLB are indicated (B).

switching mechanism responsible for the release on the inhibitory interaction between PLB and the Ca-ATPase (*14*−*16*) (Figure 1). Furthermore, while direct measurements of the interaction between PLB and the Ca-ATPase indicate that the association between the cytosolic and transmembrane domains of PLB is retained following its phosphorylation by PKA (*14*, *17*, *18*), it remains unclear whether the transmembrane or cytosolic domains of PLB may dissociate from the Ca-ATPase following enzyme activation by saturating calcium concentrations (*18*−*20*). Thus, while calcium activation of the Ca-ATPase or phosphorylation of PLB by PKA diminishes the extent of cross-linking between specific sites on the transmembrane and cytosolic domains of PLB and the Ca-ATPase, the specificity of these cross-linking reactions indicates only that a conformational rearrangement moves these sites apart and does not permit a determination of the structural change (*9*−*11*).

To identify conformational changes in the hinge structure of PLB resulting from either phosphorylation by PKA or calcium activation of the Ca-ATPase, or the possible dissociation of either the cytosolic or transmembrane domains of PLB from the Ca-ATPase, we have used an engineered PLB mutant that permits the site-specific covalent attachment of the fluorophore N-(1-pyrenyl)maleimide to Cys^{24} near the bilayer surface. Following co-reconstitution of PMal-PLB with the Ca-ATPase, the large fluorescence enhancement of PMal permits the selective measurement of PLB bound to the Ca-ATPase (*12*). Frequency-domain fluorescence resonance energy transfer (FRET) measurements of the distance between PMal bound to Cys^{24} and nitroY^{6} near the N-terminus of PLB permit the measurement of changes in the overall dimensions of the cytosolic domain of the PLB as well as possible alterations in the binding interaction with the Ca-ATPase. We report, irrespective of calcium activation of the Ca-ATPase or phosphorylation of PLB by PKA, that PLB remains associated with the Ca-ATPase in a well-defined conformation. However, the overall dimensions of the cytoplasmic portion of bound PLB increases upon calcium binding to the Ca-ATPase, whereas a more compact structure is observed following the phosphorylation of PLB by PKA, consistent with proposed models that suggest an increased helical content induced by a salt link between phospho-Ser^{16} and Arg^{13} (*16*). These results indicate that calcium binding to the Ca-ATPase overcomes conformational constraints imposed by PLB association with the nucleotide-binding domain of the Ca-ATPase; alternatively, phosphorylation of PLB by PKA induces a structural rearrangement of the cytosolic domain of PLB that releases the inhibitory interaction with the Ca-ATPase.

EXPERIMENTAL PROCEDURES

Materials. N-(1-Pyrenyl)maleimide (PMal) was obtained from Molecular Probes, Inc. (Junction City, OR). Tetranitromethane (TNM) was purchased from Alrich (Milwaukee, WI). Polyoxyethylene 9 lauryl ether ($C_{12}E_9$), cAMP-dependent protein kinase (PKA), cAMP, ATP, $MgCl_2$, the calcium ionophore A23187, EGTA, DEAE-cellulose, and *n*-octyl β-d-glucopyranoside (OG) were purchased from Sigma (St. Louis, MO). 3-(N-Morpholino)propane-sulfonic acid (MOPS) was purchased from Fisher Biotech (Fair Lawn, NJ). Bio-Beads SM2 were purchased from Bio-Rad (Richmond, CA). Cardiac SR membranes were purified as previously described (*21*). Lipids were extracted from the SR vesicles isolated from rabbit skeletal fast-twitch muscle by standard methods (*22*, *23*). The Ca-ATPase was affinity purified from skeletal muscle SR using reactive Red-agarose (*24*). DNA encoding the single cysteine mutant PLB (C36A, C41A, C46A, A24C) was cloned into a pGEX-2T plasmid expression vector and expressed in JM109 *Escherichia coli* cells as previously described (*16*, *25*). The concentration of PLB was determined by the Amido Black method (*26*). Affinity-purified PLB and Ca-ATPase were stored at −70 °C.

Specific Derivatization of PLB and Co-Reconstitution with the Ca-ATPase. The single Cys^{24} in PLB was derivatized with PMal, and when appropriate the single Tyr^{6} was selectively nitrated with TNM, as previously described in detail (*16*). Purified PLB was reconstituted in the presence of purified Ca-ATPase at a molar ratio of one PLB per Ca-ATPase into liposomes of extracted SR lipids as previously described (*12*). Following co-reconstitution with PLB, the Ca-ATPase is asymmetrically reconstituted, such that essentially all the active sites are facing outward. In contrast, PLB is symmetrically reconstituted, as assessed by both the ability of proteolytic enzymes to act upon the cytosolic domain and from a determination of the extent of phosphorylation of Ser^{16} by PKA (*17*). The 7-fold higher quantum yield of PLB in association with the cytosolic domain of the Ca-ATPase permits the preferential measurement of the fluorescence for PLB molecules that are in contact with the Ca-ATPase (*12*). Thus, the fluorescence signal used to

measure the conformation of the cytosolic portin of PLB is derived from the protein associated population of PLB, which are quantitatively phosphorylated at Ser^{16} following the addition of PKA. All protein concentrations were determined by the Amido-Black method (*26*). Free calcium concentrations were calculated from total ligand and EGTA concentrations, correcting for pH and ionic conditions (*27*).

Fluorescence Measurements. Steady-state fluorescence spectra were measured using a Spex Industries (Edison, N. J.) Fluoromax-2 spectrofluorometer. Frequency domain data (lifetime and anisotropy) were measured using an ISS K2 frequency domain fluorometer (ISS Inc., Champaign, IL), as described previously (*28*). Excitation used the 333-nm output from a Coherent (Santa Clara, CA) Innova 400 argon ion laser; emitted light was collected after a Corion interference filter (50% transmittance at 400 nm; HW = 10 nm), using 1,4-bis[5-phenyl-2-oxazolyl]-benzene (POPOP) in methanol (lifetime of 1.35 ns) as a lifetime reference. Measurements were made at 25 °C.

Analysis of Frequency-Domain Data. Explicit expressions, previously described in detail, permit the ready calculation of the lifetime components (i.e., α_i and τ_i) relating to a multiexponential decay or the Gaussian distribution of distances between donor and acceptor chromophores (*28*−*33*). In the case of FRET measurements, the incomplete nitration of Tyr^6 was taken into account, as previously described (*34*). Alternatively, algorithms are available that permit the determination of the initial anisotropy in the absence of rotational diffusion (r_o), the rotational correlation times (φ_i), and the amplitudes of the total anisotropy loss associated with each rotational correlation time ($r_0 \times g_i$), as previously described in detail (*35*, *36*). The parameter values are determined using the method of nonlinear least-squares analysis in which the reduced chi-squared (i.e., χ_R^2) are minimized (*37*). A comparison of χ_R^2 values provides a quantitative assessment of the adequacy of different assumed models to describe the data (*38*). Data were fit using the Globals software package (University of Illinois, Urbana-Champaign) or the program Mathcad (MathSoft Inc., Cambridge, MA), where errors in measurements of the phase and modulation were respectively assumed to be 0.20 and 0.005.

RESULTS

Functional Reconstitution of Engineered and Derivatized PLB with the Ca-ATPase. A single cysteine mutant of PLB was constructed in which the three wild-type transmembrane cysteines (Cys^{36}, Cys^{41}, and Cys^{46}) were substituted with alanines, and a further cysteine substitution was introduced (i.e., A24C) near the lipid-water interface (Figure 1). Following expression and purification, the PLB mutant was derivatized with the fluorophore PMal (at Cys^{24}), and Tyr^6 was nitrated with full retention of function, as previously described (*14*, *16*). Thus, these probes provide a sensitive donor−acceptor pair for FRET measurements that reflect conformational transitions affecting the spatial separation between Cys^{24} on the transmembrane sequence and Tyr^6 near the N-terminus of PLB resulting from either PKA-dependent phosphorylation of PLB or calcium activation of the Ca-ATPase.

Phosphorylation by PKA Decreases Overall Dimensions of Cytosolic Domain of PLB. Previous FRET results with this donor−acceptor pair have demonstrated that upon binding to the Ca-ATPase the cytosolic domain of PLB adopts a highly ordered and unique conformation, indicative of specific contact associations between the transmembrane and cytosolic domains of PLB and the Ca-ATPase (*12*). To investigate possible changes in the conformation of the cytosolic domain of PLB following its phosphorylation by PKA, we have used frequency-domain fluorescence spectroscopy to measure the intensity decay of PMal bound to Cys^{24} in PLB in the absence and presence of bound nitroTyr^6 following co-reconstitution with the Ca-ATPase (Figure 2). Data were collected for 20 frequencies between 0.4 and 200 MHz. Upon increasing the frequency of the exciting light, a progressive increase is observed in the phase and a decrease in the modulation of the emitted light. Following nitration

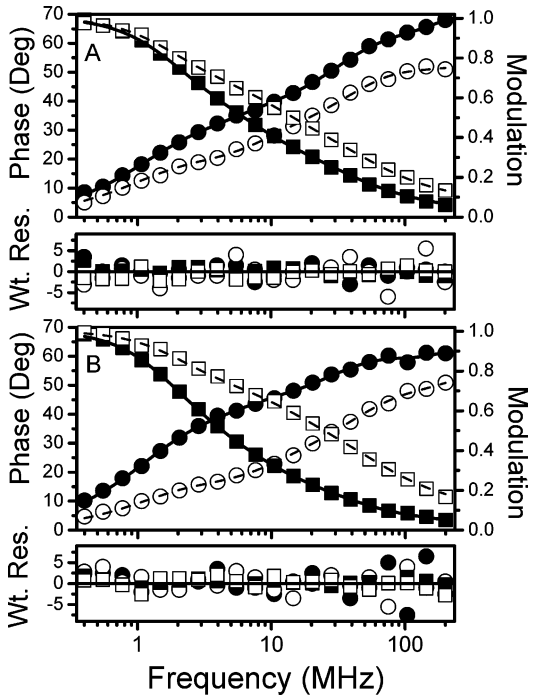

FIGURE 2: Frequency-domain lifetime data for PMal bound to PLB co-reconstituted with the Ca-ATPase before (A) and after (B) phosphorylation by PKA. Frequency-response and four-exponential fits (solid and dashed lines) corresponding to the phase shift (●, ○) and modulation (■, □) for PMal-PLB in the absence (●, ■) and presence (○, □) of the FRET acceptor nitroTyr^6. Measurements were made at 25 °C using 30 nM (0.2 μg/ml) PLB reconstituted with SR lipids in the presence of 30 nM (3 μg/ml) Ca-ATPase in 50 mM MOPS (pH 7.0), 0.1 M KCl, 5 mM $MgCl_2$, 70 μM $CaCl_2$, and 1 mM EGTA, resulting in a free calcium concentration of approximately 0.5 μM (*27*). Data were fit to a sum of four exponentials, where $I(t) = \sum_i \alpha_i e^{-t/\tau i}$ and the mean lifetime ($\bar{\tau}$) was calculated as $\sum_i \alpha_i \tau_i$. Lower panels below respective data sets represent the weighted residuals (i.e., the difference between the experimental data and the calculated fit divided by the experimental uncertainty) for models involving four-exponential fits to the data. Calculated lifetime parameters for PMal (donor only) bound to Cys^{24} in PLB were (A) $\alpha_1 = 0.47 \pm 0.01$; $\tau_1 = 0.6 \pm 0.2$ ns; $\alpha_2 = 0.36 \pm 0.02$; $\tau_2 = 4.7 \pm 0.7$ ns; $\alpha_3 = 0.12 \pm 0.02$; $\tau_3 = 20 \pm 4$ ns; $\alpha_4 = 0.050 \pm 0.002$; $\tau_4 = 95 \pm 3$ and (B) $\alpha_1 = 0.57 \pm 0.04$; $\tau_1 = 0.5 \pm 0.1$ ns; $\alpha_2 = 0.25 \pm 0.01$; $\tau_2 = 4.2 \pm 1.4$ ns; $\alpha_3 = 0.11 \pm 0.02$; $\tau_3 = 20 \pm 6$ ns; $\alpha_4 = 0.063 \pm 0.005$; $\tau_4 = 96 \pm 7$ ns. The goodness-of-fit was calculated by minimizing the χ^2_R, which minimizes the sum of the differences between the calculated and experimental values as previously described (*28*). Prior to phosphorylation by PKA, $\chi^2_R = 2.0$ (donor only) and 5.4 (donor−acceptor). Following phosphorylation by PKA, $\chi^2_R = 2.8$ (donor only) and 2.7 (donor−acceptor).

Table 1: Data from Model Involving Distribution of Distances[a]

experimental conditions[b]					
$[Ca^{2+}]_{free}$	PKA	R_o[c] (Å)	R_{av}[d] (Å)	HW[d] (Å)	χ^2_R[e]
30 nM	no	21.8 ± 0.1	14.0 (13.9−14.1)	3.7 (3.5-3.8)	5.9
0.5 μM	no	21.7 ± 0.1	15.0 (14.8−15.1)	2.7 (2.2−3.1)	6.9
0.5 μM	yes	21.5 ± 0.1	14.0 (13.9−14.1)	2.0 (1.8−2.2)	6.2
100 μM	no	21.7 ± 0.1	15.1 (14.9−15.2)	2.8 (2.2−3.3)	5.8

[a] Values and associated errors were obtained from independent measurements of FRET between PMal-Cys[24] and nitroTyr[6] in 50 mM MOPS (pH 7.0), 0.1 M KCl, 5 mM $MgCl_2$, 1 mM EGTA, and sufficient calcium yield the indicated free calcium concentration, where the fractional nitration of Tyr[6] was typically approximately 0.92. [b] Energy transfer efficiencies (*E*) represent average values and associated standard errors of the mean calculated using lifetime measurements of PMal-Cys[24] in Table 1. [c] Förster critical distance (R_o) under the indicated experimental conditions represents the distance between chromophores where the FRET efficiency is 50% (*64*, *65*). [d] Average donor−acceptor distance (R_{av}) or full-width at half-maximum (HW) assuming a Gaussian distribution of distances (*29*, *32*, *33*). Indicated errors (in brackets) were obtained from a global analysis of errors, as depicted in Figure 5. [e] Average value of reduced chi-squared (χ^2_R) fit.

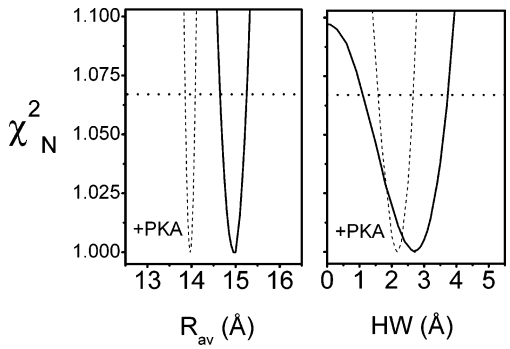

FIGURE 3: Depiction of error surfaces demonstrating conformational transition in structure of PLB following phosphorylation by PKA. Experimental curves correspond to parameter values for average donor−acceptor separation (R_{av}) and associated half-width (HW) for a model involving a Gaussian distribution of the donor−acceptor distances. Error surfaces were obtained from a global fit for three data sets for PLB co-reconstituted in the presence of the Ca-ATPase before (solid line) or after (dashed line) the phosphorylation of Ser[16] by PKA. Error surfaces were constructed by incrementally adjusting either R_{av} or HW and allowing all other parameters to vary in the least-squares analysis, which provides a conservative estimate of changes in the recovered values (*39*). The horizontal line corresponds to the *F*-statistic for one standard deviation. Experimental conditions are as described in the legend to Figure 2.

of Tyr[6] in PLB, the frequency response of PMal-PLB is shifted toward higher frequencies, indicating a reduction in the average donor lifetime due to the presence of FRET. In comparison with the untreated (inhibited) sample, the shift in the frequency response (toward higher frequencies) is much larger following the phosphorylation of PLB by PKA, indicating increased FRET upon release of the inhibitory interaction between PLB and the Ca-ATPase (Figure 2). These results, therefore, demonstrate the presence of a phosphorylation-induced decrease in the average dimensions of the cytosolic domain of PLB, consistent with earlier suggestions that phosphorylation stabilizes the secondary structure of PLB due to the formation of a salt-linkage between phosphoSer[16] and Arg[13] in PLB (*16*).

FRET Data Analysis. The intensity decay of PMal-PLB covalently bound to Cys[24] can be adequately described as a sum of four exponentials, irrespective of its phosphorylation by PKA, as indicated by the random distribution of the weighted residuals about the origin (Figure 2). Including additional fitting parameters made no further improvement in the goodness-of-fit. Assuming a single unique conformation of PLB, the decrease in average lifetime (i.e., $\bar{\tau}$) is often used to calculate an apparent spatial separation. However, this model does not take into account protein structural heterogeneity and provides no information regarding possible changes in conformational heterogeneity that may be associated with interactions between PLB and multiple binding sites on the Ca-ATPase or the dissociation of either the transmembrane or cytosolic domain of PLB from the Ca-ATPase. We have, therefore, fit the data to a model involving a distribution of distances that explicitly takes into account protein conformational heterogeneity and provides an equivalent fit (based on a consideration of the residuals and χ^2_R) to the lifetime data with fewer floating parameters (Table 1) (*12*, *16*, *29*, *32*).

A consideration of the error surfaces for these calculated distance distributions provides a conservative estimate of the recovered parameters (*39*) and demonstrates the presence of two well-defined conformations for the cytoplasmic portion of PLB both before and after phosphorylation of Ser[16] by PKA (Figure 3). Before phosphorylation by PKA, the average distance (R_{av}) between PMal at Cys[24] and nitroTyr[6] within bound PLB is 15.0 ± 0.2 Å (Figure 3A). Following phosphorylation by PKA, the R_{av} is 14.0 ± 0.1 Å. Irrespective of phosphorylation by PKA, the half-width of the distribution is approximately 2−3 Å (Figure 3B), indicative of specific binding interactions between PLB and the Ca-ATPase that define a unique conformation of the cytosolic domain of PLB. In contrast, the average spatial separation between these chromophores is poorly determined for PLB reconstituted in the absence of the Ca-ATPase (i.e., R_{av} < 21 Å; HW = 36 Å); the large half-width indicates the presence of a flexible hinge region between the transmembrane and cytosolic domains of PLB (*16*, *40*). Thus, the narrow distance distributions are indicative of conformationally distinct structures of PLB bound to the Ca-ATPase before and after phosphorylation by PKA. These results provide the first indication that the structure of PLB is well-defined following the release of enzyme inhibition by the PKA-dependent phosphorylation of PLB. In addition, these results confirm earlier suggestions that the cytosolic and transmembrane domains of PLB remain associated with the Ca-ATPase following phosphorylation by PKA and the release of enzyme inhibition (*14*, *17*, *18*). Thus, PLB appears to regulate Ca-ATPase function through modest conformational changes consistent with other known allosteric modulators of enzyme function.

Localized Structural Changes Near Putative Hinge Upon PLB Phosphorylation. To further assess possible changes in the structure of PLB upon release of Ca-ATPase inhibition following phosphorylation by PKA, we have measured the rotational dynamics of PMal covalently bound to Cys[24] in the transmembrane domain of PLB using frequency-domain fluorescence anisotropy methods. The differential phase and modulated anisotropy were measured over 20 frequencies between 0.4 and 200 MHz for PMal-PLB before and after

Table 2: Rotational Dynamics of PMal Bound to Cys[24] in PLB[a]

experimental conditions[b]								
$[Ca^{2+}]_{free}$	PKA	r_o	$g_1 \times r_o$	φ_1 (ns)	$g_2 \times r_o$	φ_2 (ns)	r_∞	χ^2_R[c]
30 nM	no	0.29 (0.23−0.40)	0.10 (0.08−0.15)	0.8 (0.2−1.4)	0.05 (0.03−0.07)	17 (12−23)	0.14 (0.11−0.16)	5.1
0.5 μM	no	0.29 (0.25−0.31)	0.10 (0.09−0.11)	0.7 (0.4−1.3)	0.047 (0.041−0.053)	11 (7−14)	0.140 (0.132−0.153)	6.4
0.5 μM	yes	0.30 (0.25−0.40)	0.15 (0.11−0.20)	0.5 (0.2−0.8)	0.04 (0.02−0.07)	24 (13−38)	0.10 (0.07−0.12)	3.5
100 μM	no	0.34 (0.28−0.40)	0.16 (0.13−0.19)	0.5 (0.3−0.8)	0.049 (0.045−0.052)	8 (6−10)	0.13 (0.11−0.16)	3.8

[a] Mean values and associated standard errors of the mean (in brackets) obtained from a four-exponential fit to frequency-domain data collected for PMal bound to Cys[24], as described in the legend to Figure 5. [b] Associated errors (in parentheses) obtained from error surfaces associated with simultaneous fits to three independent measurements obtained from a global fit to three data sets (*39*).

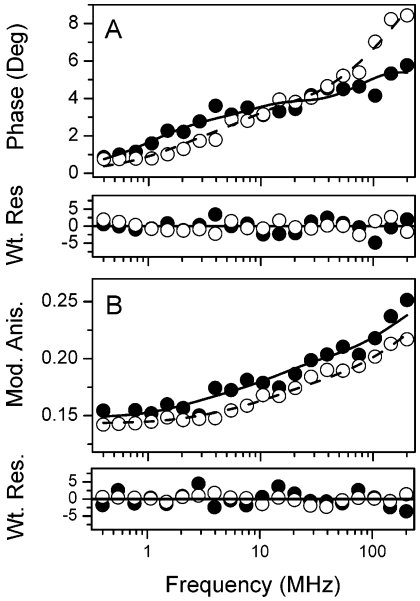

FIGURE 4: Fluorescence anisotropy decays for PMal-PLB co-reconstituted with the Ca-ATPase before (●, —) or after (○, ---) phosphorylation by PKA. Measured differential phase angles (A) and modulated anisotropies (B) and associated nonlinear least-squares fits to multiexponential model (—, ---) are shown, where $r(t) = (r_o - r_\infty)\sum_{i=1}^{n} g_i \exp^{-(t/\phi i)} + r_\infty$. r_o and r_∞ are the limiting anisotropy in the absence and presence of rotational diffusion, φ_i are the rotational correlation times, and $g_i \times r_o$ represent the amplitudes associated of the total anisotropy loss associated with each rotational correlation time. The weighted residuals (Wt. Res.) are shown below respective data sets. Experimental conditions are as described in the legend to Figure 2.

phosphorylation (Figure 4). A progressive increase in both the differential phase and modulated anisotropy is observed as the frequency increases. While there are small differences, the overall shape of the frequency responses for PLB bound to the Ca-ATPase are very similar, indicating that the rates of motion are not significantly affected by the phosphorylation of PLB by PKA. A nonlinear least-squares fit of the data requires a model involving two rotational rates (i.e., φ_1 and φ_2) and a residual anisotropy (i.e., r_∞) (Table 2), which correspond to segmental rotational motions of PMal (i.e., φ_1), changes in the backbone motions of the transmembrane domain (i.e., φ_2), and conformational restrictions imposed upon PLB by the membrane bilayer and Ca-ATPase (i.e., r_∞). As previously described, the rates of independent probe motion (i.e., φ_1) and dynamic fluctuations of the protein backbone (i.e., φ_2) are not significantly affected by association with the Ca-ATPase (*12*). Rather, the amplitudes associated with each rotational rate are affected, such that the contribution of faster motions associated with backbone fluctuations of PLB are reduced upon binding to the Ca-ATPase. These results are consistent with the location of PMal at Cys[24], which has been shown to be located in a conformationally disordered region of PLB that does not undergo direct contact interactions with the Ca-ATPase (*14*). The reduction in the amplitude of motion associated with the backbone-fold (i.e., $g_2 \times r_o$), which varies from 0.10 ± 0.01 for PLB alone to 0.05 ± 0.01 following association with the Ca-ATPase, is diagnostic of the interaction between PLB and the Ca-ATPase (*12*). In the current manuscript, the amplitude of motion associated with the backbone-fold of PLB does not change (i.e., $g_2 \times r_o = 0.05$) irrespective of phosphorylation of PLB by PKA or calcium activation of the Ca-ATPase (Table 2). These results provide strong evidence that PLB remains associated with the Ca-ATPase under all conditions studied in this manuscript.

The only significant change in the fitting parameters following PLB phosphorylation is the amplitude associated with probe mobility, which is slightly increased following the phosphorylation by PKA and results in a decrease in the residual anisotropy (r_∞). Thus, there are localized changes in the structure of PLB near the putative hinge, in agreement with earlier observations that implicate this structural element as a conformational switch that modulates the inhibitory interaction between PLB and the Ca-ATPase (*14*−*16*). However, the transmembrane domain of PLB remains tightly associated with the Ca-ATPase following phosphorylation of PLB by PKA.

Calcium Activation of the Ca-ATPase Increases the Overall Dimensions of the Cytosolic Domain of PLB. Differences in the structural interactions between PLB and Ca-ATPase have been observed to result from calcium activation or the phosphorylation of PLB by PKA. For example, PLB remains associated with the Ca-ATPase following immunoprecipitation of the detergent-solubilized Ca-ATPase irrespective of whether PLB is phosphorylated by PKA; on the other hand, the complex between PLB and the Ca-ATPase does not coprecipitate upon calcium activation of the Ca-ATPase (*18*). However, the structural basis of alterations in the binding interaction between PLB and the Ca-ATPase following detergent solubilization remains unclear; in membrane bilayers PLB remains associated with the Ca-ATPase following calcium activation (*20*). Yet, the site-specific chemical cross-linking between engineered sites on PLB and the Ca-ATPase are diminished following

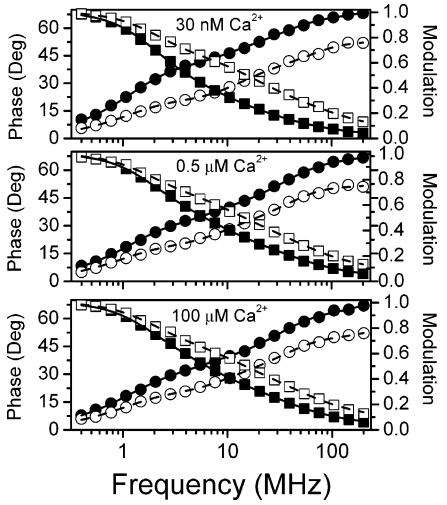

FIGURE 5: Frequency-domain lifetime data for PMal bound to PLB co-reconstituted with the Ca-ATPase in the presence of the indicated free calcium concentrations. Frequency-response and four-exponential fits (solid and dashed lines) corresponding to the phase shift (●, ○) and modulation (■, □) for PMal-PLB in the absence (●, ■) and presence (○, □) of the FRET acceptor nitroTyr[6]. Measurements were made at 25 °C using 30 nM (0.2 μg/ml) PLB reconstituted with SR lipids in the presence of 30 nM (3 μg/ml) Ca-ATPase in 50 mM MOPS (pH 7.0), 0.1 M KCl, 5 mM $MgCl_2$, 1 mM EGTA, and sufficient calcium to yield the indicated free calcium concentration (*27*). Data were fit to a sum of four exponentials, where $I(t) = \sum_i \alpha_i e^{-t/\tau i}$ and the mean lifetime ($\bar{\tau}$) was calculated as $\sum_i \alpha_i \tau_i$. Calculated lifetime parameters for PMal (donor only) bound to Cys[24] in PLB were (top) $\alpha_1 = 0.45 \pm 0.01$; $\tau_1 = 0.5 \pm 0.1$ ns; $\alpha_2 = 0.28 \pm 0.01$; $\tau_2 = 4.2 \pm 0.4$ ns; $\alpha_3 = 0.17 \pm 0.01$; $\tau_3 = 16 \pm 1$ ns; $\alpha_4 = 0.095 \pm 0.006$; $\tau_4 = 95 \pm 1$, (middle) $\alpha_1 = 0.47 \pm 0.01$; $\tau_1 = 0.6 \pm 0.2$ ns; $\alpha_2 = 0.36 \pm 0.02$; $\tau_2 = 4.7 \pm 0.7$ ns; $\alpha_3 = 0.12 \pm 0.02$; $\tau_3 = 20 \pm 4$ ns; $\alpha_4 = 0.050 \pm 0.002$; $\tau_4 = 95 \pm 3$, and (bottom) $\alpha_1 = 0.49 \pm 0.03$; $\tau_1 = 0.6 \pm 0.1$ ns; $\alpha_2 = 0.35 \pm 0.02$; $\tau_2 = 4.7 \pm 0.6$ ns; $\alpha_3 = 0.11 \pm 0.02$; $\tau_3 = 19 \pm 4$ ns; $\alpha_4 = 0.047 \pm 0.006$; $\tau_4 = 92 \pm 6$ ns. The goodness-of-fit was calculated by minimizing the χ^2_R, which minimizes the sum of the differences between the calculated and experimental values as previously described (*33*), and χ^2_R equals: (top) 2.8 (donor only) and 2.7 (donor−acceptor), (middle) 2.0 (donor only) and 4.2 (donor−acceptor), and (bottom) 2.7 (donor only) and 3.2 (donor−acceptor).

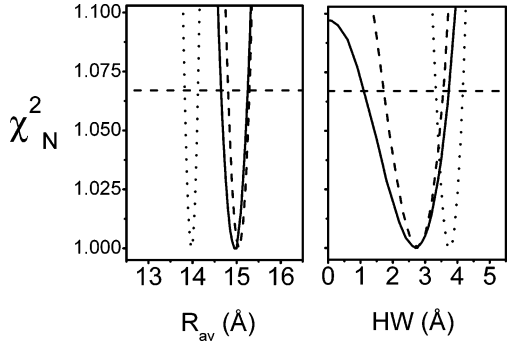

FIGURE 6: Depiction of error surfaces demonstrating conformational transition in structure of PLB following calcium binding to Ca-ATPase. Experimental curves correspond to free calcium levels of 30 nM (dotted line), 0.5 μM (solid line), and 100 μM (dashed line). The horizontal line corresponds to the *F*-statistic for one standard deviation. Experimental conditions are as described in the legend to Figure 5.

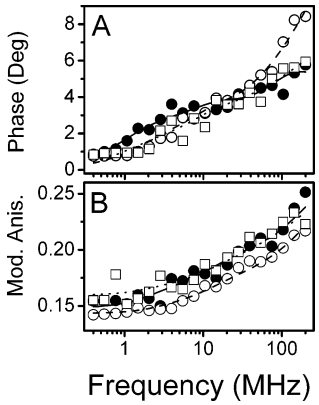

FIGURE 7: Measured differential phase angles (A) and modulated anisotropy (B) data (●, □, ○) and nonlinear least-squares fits (—, ····, ---) of the rotational dynamics of PMal-PLB co-reconstituted with the Ca-ATPase at variable free calcium concentrations, where the free calcium concentrations are 30 nM (●, solid line), 0.5 μM (□, dotted line), and 100 μM (○, dashed line). Experimental conditions are as described in the legend to Figure 5.

calcium activation of the Ca-ATPase (*9*−*11*, *41*), suggesting a movement of these sites with respect to one another. Therefore, to better understand the mechanism underlying the reduced calcium sensitivity of Ca-ATPase activity when PLB is bound, we have measured the dimensions of the cytosolic portion of bound PLB as a function of the free calcium concentration (Figure 5).

We find that before calcium activation (i.e., 30 nM free calcium), significant energy transfer occurs between PMal (Cys[24]) and Tyr[6], as evidenced by the large shift in the frequency response of PMal-PLB bound to the Ca-ATPase (i.e., donor only) upon nitration of Tyr[6] (i.e., donor−acceptor) (Figure 5). Calcium binding to the Ca-ATPase results in a significant reduction in the shift of the frequency response of donor−acceptor relative to donor-only, indicating reduced energy transfer and a larger spatial separation between PMal bound to Cys[24] and nitroTyr[6] following calcium activation of the Ca-ATPase. Both nonsaturating (i.e., 0.5 μM) and saturating (i.e., 100 μM) free calcium concentrations result in similar reduced energy transfer efficiencies in comparison to the apo-enzyme, suggesting that occupancy of high-affinity calcium-binding site(s) of the Ca-ATPase is sufficient to induce the observed conformational rearrangement of PLB (*1*, *42*). Irrespective of the calcium concentration, the conformational heterogeneity of the cytosolic domain of PLB (as measured by the width of the distance distribution) remains narrow, indicating specific binding interactions between the cytosolic and transmembrane domains of PLB with the Ca-ATPase (Figure 6). Thus, while phosphorylation of Ser[16] stabilizes the backbone-fold of PLB to bring the labeled residues into closer proximity, calcium activation of the Ca-ATPase induces structural changes within the Ca-ATPase that, in turn, induces a more extended conformation of PLB.

Altered Structural Interaction with PLB Upon Calcium Activation of the Ca-ATPase. The frequency response of the modulated anisotropy and differential phase of PMal-PLB in association with the Ca-ATPase was measured to detect calcium-induced alterations in the structural interaction between PLB and the Ca-ATPase. Calcium activation of the Ca-ATPase results in a small change in the anisotropy decay (Figure 7), which is the result of a small increase in the amplitude of segmental probe motion and an increase in the rate of backbone dynamics (Table 2**)**. The change in the frequency response of the anisotropy decay of PMal-PLB

upon calcium activation is very similar to that observed upon the phosphorylation of PLB by PKA (Figure 4), suggesting similar structural changes in the vicinity of the putative hinge element occur irrespective of the mechanism of Ca-ATPase activation.

DISCUSSION

To identify the mechanism of PLB inhibition that results in a shift in the calcium-dependence of Ca-ATPase activation and how phosphorylation of PLB by PKA releases this inhibition, we have probed the overall dimensions and conformational heterogeneity of the cytosolic portion of PLB bound to the Ca-ATPase using fluorescence spectroscopy. In contrast to the large range of conformations (HW = 36 Å) adopted for the cytosolic portion of PLB reconstituted in the absence of the Ca-ATPase, we find that the conformation is well defined when PLB is bound to the Ca-ATPase (i.e., the half-width of the distance distribution is approximately 3 Å). The large decrease in HW upon binding to the Ca-ATPase is consistent with FRET measurements of other proteins that adopt well-defined structures upon association with their binding partners (*43*, *44*). These highly ordered binding interactions between PLB and the Ca-ATPase are retained following either phosphorylation by PKA or calcium activation of the Ca-ATPase. Thus, in conjunction with fluorescence anisotropy measurements of restricted rotational dynamics under the same conditions (Figures 4 and 7), it is apparent that both the transmembrane and cytosolic domains of PLB remain tightly associated with the Ca-ATPase. Thus, the nature of the conformational switch that underlies release of Ca-ATPase inhibition does not involve the dissociation of either domain of PLB from the Ca-ATPase.

Moreover, the retention of similar dimensions for the cytosolic portion of PLB (14−15 Å), irrespective of calcium activation or the phosphorylation of PLB, suggests localized structural changes that selectively destabilize the inhibitory interaction between PLB and the Ca-ATPase. The phosphorylation-induced decrease in spatial separation between PMal covalently bound to Cys^{24} and nitroTyr^{6} is consistent with a mechanism involving α-helical stabilization within PLB by a salt bridge between the phosphoryl group at Ser^{16} and the guanidine moiety of Arg^{13}, which was previously suggested to modulate the hinge mobility of PLB reconstituted in the absence of the Ca-ATPase (*16*) (Figure 8).

In contrast, the inhibition of the Ca-ATPase by PLB, which is manifested in a shift in the calcium-dependence of Ca-ATPase activation toward higher calcium concentrations, can be understood in terms of the kinetics of calcium activation. Prior equilibrium binding measurements have revealed that PLB does not affect the calcium-dependence (affinity) of calcium binding (*1*). Rather, PLB selectively modulates the energetics of the cooperative structural change (i.e., $E_{Ca} \rightarrow E'_{Ca}$) associated with the formation of the second high-affinity calcium binding site within the Ca-ATPase (Scheme 1) (*1*, *21*). This latter result is consistent with prior kinetic measurements that, in conjunction with the high-resolution structure of the Ca-ATPase, indicate formation of the second calcium binding site is the rate-limiting process underlying calcium activation and ATP utilization by the Ca-ATPase (*42*, *45*−*48*). Thus, when PLB is complexed with the Ca-ATPase, occupancy of the first calcium binding site induces a conformational change of the Ca-ATPase that allows binding of the second calcium; this conformational change coincides with the extension of the cytosolic domain of bound

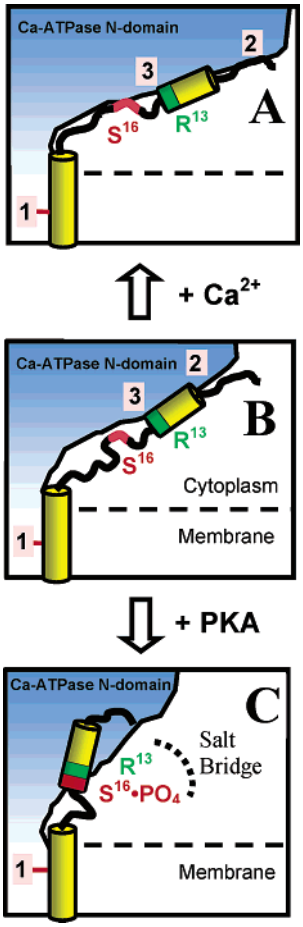

FIGURE 8: Model depicting relationship between formation of salt-linkage between phosphoSer^{16} and Arg^{13} in PLB and release of inhibitory interaction between the cytosolic domain of PLB (yellow) and nucleotide binding domain (N-domain) of the Ca-ATPase (blue). The cartoon takes into account cross-linking derived interaction sites between the transmembrane domain of PLB (N^{27} and N^{30}) and the transmembrane helix M4 of the Ca-ATPase (i.e., L^{321} and C^{318}) (site 1) as well as K^3 near the amino-terminus of PLB and the $KDDKPVK^{403}$ binding sequence (site 2) within the N-domain of the Ca-ATPase (*9*−*11*, *63*). In addition, a putative regulatory interaction between PLB and the Ca-ATPase (site 3) is depicted that may involve a salt linkage between Arg^{13} within PLB and acidic residues within the nucleotide binding domain of the Ca-ATPase (A, B). Prior to its phosphorylation by PKA, the hinge region within PLB assumes an extended structure, permitting association of the cytosolic domain of PLB with sites 2 and 3 on the nucleotide-binding domain of the Ca-ATPase (A, B). This binding interaction induces a reorientation of the nucleotide-binding domain of the Ca-ATPase by approximately 10° to bring the PLB binding sequence closer to the membrane surface (B) (*5*, *12*). PLB binding functions to increase the energetic barriers associated with the rigid body reorientation of the N-domain that accompanies calcium activation of the Ca-ATPase (A), shifting the calcium-dependence of ATPase activity toward higher calcium concentrations (*5*, *13*, *49*). In contrast, phosphorylation of Ser^{16} by PKA induces the formation of a salt-linkage with Arg^{13} (dashed line in panel C), constraining the overall dimensions of the cytosolic portion of PLB by stabilizing the helical structure of the hinge region (bottom figure; see Figure 1). As a result, the cytoplasmic portion of PLB releases the inhibitory interaction with sites 2 and 3, which is associated with a physical constraint of the N-domain and enzyme inhibition, and binds to an as yet unidentified sequence of the Ca-ATPase.

Scheme 1

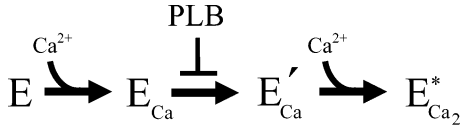

PLB. We suggest that, in its unphosphorylated state, bound PLB constrains the structure of the Ca-ATPase so that the rate of this conformational transition is reduced; higher calcium concentrations are necessary to overcome the kinetic barrier associated with the cooperative binding of the second calcium ion. Thus, the larger kinetic barrier associated with the formation of the second high-affinity calcium binding site results in a reduced calcium sensitivity, limiting the rate of calcium sequestration, since occupancy of the second high-affinity calcium site is necessary to promote ATP activation and phosphoenzyme formation. Further, the calcium-dependent reorientation of both the transmembrane helices of the Ca-ATPase and individual cytosolic domains is consistent with observed reductions in site-specific chemical cross-linking between engineered sites on the Ca-ATPase and PLB following calcium activation (*9*−*11*, *41*).

This mechanism involving inhibition of catalytically important movements of the Ca-ATPase by PLB is consistent with the previous structural data regarding the interaction between the cytoplasmic domain of PLB and the nucleotide binding domain of the Ca-ATPase, which demonstrates that PLB binding alters both the orientation of the nucleotide binding domain and restricts that rate of domain movement (*5*, *9*, *21*). Thus, it is expected that PLB binding will affect calcium-induced large-scale domain movements of the nucleotide-binding domain that are normally associated with enzyme activation (*13*, *48*, *49*). Since these protein domain movements are critical to transport function and have previously been shown to be rate limiting under physiological conditions, a restriction of domain mobility is expected to reduce the overall rate of calcium transport function (*5*, *21*, *50*−*53*). Indeed, other physiological modulators of Ca-ATPase function beside PLB expression, including changes in lipid composition, directly modulate activity through the modulation of dynamics of the nucleotide binding domain (*5*, *54*, *55*).

Thus, our results suggest that PLB functions as an allosteric regulator of the Ca-ATPase, where the structure of the hinge region modulates the inhibitory interaction between PLB and the Ca-ATPase. Prior to the release of the inhibitory interaction between PLB and the Ca-ATPase, the hinge region within PLB assumes a more extended structure (Figure 8), permitting the association between sequences within the cytosolic domain IA of PLB with the inhibitory sequence of the Ca-ATPase associated with enzyme inhibition (Figure 1). This interaction requires a reorientation of the nucleotide-binding domain of the Ca-ATPase to bring the PLB binding sequence closer to the membrane surface (*12*). The associated restriction in the mobility of the nucleotide binding domain functions to inhibit the transport kinetics of the Ca-ATPase (*5*, *13*). Upon phosphorylation of Ser^{16}, a salt-linkage is formed with Arg^{13}, which functions to constrain the overall dimensions of the cytosolic domain of PLB by stabilizing the secondary structure within the hinge region. Release of the inhibitory interaction between PLB and the Ca-ATPase must be understood in the context of the extended and motionally restricted structures of PLB and the Ca-ATPase, which is released by the disruption of the inhibitory interaction through the translational movement of the cytosolic region of PLB.

Our results, which demonstrate that PLB remains associated with the Ca-ATPase following the release of enzyme inhibition, are in agreement with all prior measurements that have directly probed the structural interaction between PLB and the Ca-ATPase (*14*, *17*, *20*, *56*). Using NMR, FTIR, spin-label EPR, and fluorescence spectroscopy, it has been demonstrated that structural interactions between both the cytosolic and transmembrane domains of PLB and the Ca-ATPase are retained following either phosphorylation of PLB by PKA or calcium activation of the Ca-ATPase. Following calcium activation the high-affinity binding interaction between PLB and the Ca-ATPase has been measured (i.e., $K_d = 140 \pm 30\ \mu M$) (*20*). The functional inhibition of Ca-ATPase activity mirrors the extent of PLB binding in both native and reconstituted preparations (*2*). Thus, irrespective of the calcium concentration, $70 \pm 6\%$ of the total PLB is bound to the Ca-ATPase in slow-twitch skeletal muscle or following the functional co-reconstitution of equal molar amounts of PLB and the Ca-ATPase (*2*, *20*). Nevertheless, models of Ca-ATPase regulation that involve dissociation of PLB from the Ca-ATPase upon either calcium activation of the Ca-ATPase or phosphorylation of PLB by PKA are commonly proposed in the current literature (*6*, *10*, *41*). For example, Jones and co-workers have suggested that PLB dissociates from the Ca-ATPase following calcium activation on the time-scale of enzymatic turnover, and propose that PLB dissociation induces the disruption of large dodecameric aggregates of the Ca-ATPase to enhance the transport activity of the pump (*19*, *41*, *57*). This latter model suggests a cycle of PLB dissociation and rebinding during the catalytic transport cycle of the pump and on a beat-to-beat basis during contraction, irrespective of the extent of beta-adrenergic receptor activation (*41*).

Models of Ca-ATPase regulation by PLB that involve the complete dissociation of PLB from the Ca-ATPase are largely derived from the observation that site-specific cross-linking reactions between residues on PLB and the Ca-ATPase are diminished upon either calcium activation of the Ca-ATPase or phosphorylation of PLB by PKA (*9*, *10*, *41*). However, changes in cross-linking efficiency are not able to distinguish between dissociation of PLB from the Ca-ATPase relative to other models in which the specific reactive groups on either PLB or the Ca-ATPase need only reorient or move apart small distances to diminish the efficiency of the cross-linking reaction, as documented previously (*41*). Indeed, the structure of a primary cross-linking site on the Ca-ATPase (i.e., K^{328}), located at the C-terminus of the M4 helix in the calcium-activated form of the pump (1EUL.pdb), is altered in the apo-forms of the Ca-ATPase (1IWO.pdb and 1KJU.pdb) (*48*, *49*, *59*). Thus, changes in the orientation and secondary structures of the transmembrane helices of the Ca-ATPase that occur upon calcium activation are consistent with observed changes in cross-linking efficiency between PLB and the Ca-ATPase (*48*, *58*). In fact, cross-linking interactions between PLB and the Ca-ATPase are retained following the phosphorylation of PLB by PKA, and are optimal only for the apo-form of the Ca-ATPase in the

presence of bound nucleotide (*10*, *41*). In this respect, the identification of conditions that optimize the site-specific cross-linking between sites on PLB and the Ca-ATPase can most effectively be used to constrain possible structural interactions between PLB and the Ca-ATPase, rather then inferring global changes in the structures of either PLB or the Ca-ATPase (*11*, *16*, *60*).

Additional support for models that suggest the dissociation of PLB to underlie the functional regulation of the Ca-ATPase in the heart have been inferred from early measurements using phosphorescence anisotropy to monitor the structure of the Ca-ATPase (*57*). These measurements have been interpreted to suggest that PLB induces the formation of large dodecameric oligomers of the Ca-ATPase that are functionally inactive (*19*, *61*). The dissociation of PLB from these large oligomers of the Ca-ATPase following phosphorylation by PKA was proposed to enhance enzyme activity through the dissociation of these large aggregates of the Ca-ATPase. However, observed large changes in the phosphorescence anisotropy of the erythrosin probe bound to the Ca-ATPase following the phosphorylation of PLB was subsequently shown to be the result of the high stoichiometry of the bound dye, which has the potential to induce changes in phosphorescence depolarization through intramolecular energy transfer due to changes in the proximity of nearby labels (*5*, *13*). Using lower labeling stoichiometries that permit the selective labeling of the nucleotide-binding domain of the Ca-ATPase, PLB binding was shown to have no affect on the oligomeric state of the Ca-ATPase (*5*). Rather, PLB binding induces alterations in the relative orientation of the nucleotide-binding domain to modify the calcium-dependence of enzymatic activity (*5*, *12*, *13*, *21*). Under these latter conditions, both the cytosolic and transmembrane domains of PLB remain associated with the Ca-ATPase (*14*, *17*). Thus, there is no reliable data to support earlier models that suggested the dissociation of PLB is required to release the inhibition of Ca-ATPase activity.

In addition to confirming earlier measurements that PLB remains associated with the Ca-ATPase following the release of inhibition through either the direct phosphorylation of PLB by PKA or calcium activation of the Ca-ATPase, the current results further clarify the structure of PLB in association with Ca-ATPase. Specifically, we demonstrate that PLB assumes a unique conformation when bound to the Ca-ATPase irrespective of the release of enzyme inhibition following the phosphorylation of PLB by PKA or calcium activation of the Ca-ATPase. Indeed, it is the stabilization of the hinge element of PLB following phosphorylation of Ser^{16} by PKA that functions as an important conformational switch to release the inhibitory interactions between the cytoplasmic domain of PLB and the nucleotide-binding domain of the Ca-ATPase, which enhances the kinetics of calcium activation and transport function through the modulation of catalytically important domain motions of the Ca-ATPase (*1*, *5*, *12*, *13*, *16*, *54*, *55*, *62*).

REFERENCES

1. Cantilina, T., Sagara, Y., Inesi, G., and Jones, L. R. (1993) Comparative studies of cardiac and skeletal sarcoplasmic reticulum ATPases. Effect of a phospholamban antibody on enzyme activation by Ca^{2+}, *J. Biol. Chem. 268*, 17018−17025.
2. Ferrington, D. A., Yao, Q., Squier, T. C., and Bigelow, D. J. (2002) Comparable levels of Ca-ATPase inhibition by phospholamban in slow-twitch skeletal and cardiac sarcoplasmic reticulum, *Biochemistry 41*, 13289−13296.
3. Tada, M., Kirchberger, M. A., and Katz, A. M. (1975) Phosphorylation of a 22, 000-dalton component of the cardiac sarcoplasmic reticulum by adenosine 3′:5′-monophosphate-dependent protein kinase, *J. Biol. Chem. 250*, 2640−2647.
4. Inui, M., Chamberlain, B. H., Saito, A., and Fleischer, S. (1986) The nature of the modulation of Ca^{2+} transport as studied by reconstitution of cardiac sarcoplasmic reticulum, *J. Biol. Chem. 261*, 1794−1800.
5. Negash, S., Huang, S., and Squier, T. C. (1999) Rearrangement of domain elements of the Ca-ATPase in cardiac sarcoplasmic reticulum membranes upon phospholamban phosphorylation, *Biochemistry 38*, 8150−8158.
6. MacLennan, D. H., and Kranias, E. G. (2003) Phospholamban: a crucial regulator of cardiac contractility, *Nat. Rev. Mol. Cell Biol. 4*, 566−577.
7. Berridge, M. J., Bootman, M. D., and Roderick, H. L. (2003) Calcium signaling: dynamics, homeostasis and remodeling, *Nat. Rev. Mol. Cell Biol. 4*, 517−529.
8. MacLennan, D. H., Kimura, Y., and Toyofuku, T. (1998) Sites of regulatory interaction between calcium ATPases and phospholamban, *Ann. N.Y. Acad. Sci. 853*, 31−42.
9. James, P., Inui, M., Tada, M., Chiesi, M., and Carafoli, E. (1989) Nature and site of phospholamban regulation of the Ca^{2+} pump of sarcoplasmic reticulum, *Nature 342*, 90−92.
10. Jones, L., Cornea, R. L., and Chen, Z. (2002) Close proximity between residue 30 of phospholamban and cysteine 318 of the cardiac Ca2+ pump revealed by intermolecular thiol cross-linking, *J. Biol. Chem. 277*, 28319−28329.
11. Toyoshima, C., Asahi, M., Sugita, Y., Khanna, R., Tsuda, T., and MacLennan, D. H. (2003) Modeling of the inhibitory interaction of phospholamban with the Ca2+ ATPase, *Proc. Natl. Acad. Sci. U.S.A. 100*, 467−472.
12. Li, J., Xiong, Y., Bigelow, D. J., and Squier, T. C. (2004) Phospholamban binds in a compact and ordered conformation to the Ca-ATPase, *Biochemistry 43*, 455−463.
13. Huang, S., and Squier, T. C. (1998) Enhanced rotational dynamics of the phosphorylation domain of the Ca-ATPase upon calcium activation, *Biochemistry 37*, 18064−18073.
14. Chen, B., and Bigelow, D. J. (2002) Phosphorylation induces a conformational transition near the lipid-water interface of phospholamban reconstituted with the Ca-ATPase, *Biochemistry 41*, 13965−13972.
15. Hughes, E., and Middleton, D. A. (2003) Solid-state NMR reveals structural changes in phospholamban accompanying the functional regulation of Ca^{2+}-ATPase, *J. Biol. Chem. 278*, 20835−20842.
16. Li, J., Bigelow, D. J., and Squier, T. C. (2003) Phosphorylation by cAMP-dependent protein kinase modulates the structural coupling between the transmembrane and cytosolic domains of phospholamban, *Biochemistry 42*, 10674−10682.
17. Negash, S., Yao, Q., Sun, H., Li, J., Bigelow, D. J., and Squier, T. C. (2000) Phospholamban remains associated with the Ca2+- and Mg2+-dependent ATPase following phosphorylation by cAMP-dependent protein kinase, *Biochem. J. 351*, 195−205.
18. Asahi, M., McKenna, E., Kurzydlowski, K., Tada, M., and MacLennan, D. H. (2000) Physical interactions between phospholamban and sarco(endo)plasmic reticulum Ca^{2+}-ATPases are dissociated by elevated Ca^{2+}, but not by phospholamban phosphorylation, vanadate, or thapsigargin, and are enhanced by ATP, *J. Biol. Chem. 275*, 15034−15038.
19. Thomas, D. D., Reddy, L. G., Karim, C. B., Li, M., Cornea, R., Autry, J. M., Jones, L. R., and Stamm, J. (1998) Direct spectroscopic detection of molecular dynamics and interactions of the calcium pump and phospholamban, *Ann. N.Y. Acad. Sci. 853*, 186−194.
20. Tatulian, S. A., Chen, B., Li, J., Negash, S., Middaugh, C. R., Bigelow, D. J., and Squier, T. C. (2002) The inhibitory action of phospholamban involves stabilization of alpha-helices within the Ca-ATPase, *Biochemistry 41*, 741−751.
21. Negash, S., Chen, L. T., Bigelow, D. J., and Squier, T. C. (1996) Phosphorylation of phospholamban by cAMP-dependent protein kinase enhances interactions between Ca-ATPase polypeptide chains in cardiac sarcoplasmic reticulum membranes, *Biochemistry 35*, 11247−11258.
22. Chen, P. S., Toribara, T. Y., and Warner, H. (1965) Microdetermination of phosphorus, *Anal. Chem. 28*, 1756−1758.

23. Fernandez, J. L., Rosemblatt, M., and Hidalgo, C. (1980) Highly purified sarcoplasmic reticulum vesicles are devoid of Ca^{2+}-independent ('basal') ATPase activity, *Biochim. Biophys. Acta 599*, 552−568.
24. Yao, Q., Chen, L. T., and Bigelow, D. J. (1998) Affinity purification of the Ca-ATPase from cardiac sarcoplasmic reticulum membranes, *Protein Expression Purif. 13*, 191−197.
25. Yao, Q., Bevan, J. L., Weaver, R. F., and Bigelow, D. J. (1996) Purification of porcine phospholamban expressed in *Escherichia coli*, *Protein Expression Purif. 8*, 463−468.
26. Schaffner, W., and Weissmann, C. (1973) A rapid, sensitive, and specific method for the determination of protein in dilute solution, *Anal. Biochem. 56*, 502−514.
27. Fabiato, A. (1988) Computer programs for calculating total from specified free or free from specified total ionic concentrations in aqueous solutions containing multiple metals and ligands, *Methods Enzymol. 157*, 378−417.
28. Hunter, G. W., and Squier, T. C. (1998) Phospholipid acyl chain rotational dynamics are independent of headgroup structure in unilamellar vesicles containing binary mixtures of dioleoylphosphatidylcholine and dioleoyl-phosphatidylethanolamine, *Biochim. Biophys Acta 1415*, 63−76.
29. Haas, E., Katchalski-Katzir, E., and Steinberg, I. (1978) Effect of the orientation of donor and acceptor on the probability of energy transfer involving electronic transitions of mixed polarization, *Biochemistry 17*, 5064−5070.
30. Weber, G. (1981) Resolution of the fluorescence lifetimes in a heterogeneous system by phase and modulation measurements, *J. Phys. Chem. 85*, 949−953.
31. Beechem, J. M., and Haas, E. (1989) Simultaneous determination of intramolecular distance distributions and conformational dynamics by global analysis of energy transfer measurements, *Biophys. J. 55*, 1225−1236.
32. Cheung, H. C. (1991) Resonance Energy Transfer, in Topics in Fluorescence Spectroscopy (Lakowicz, J. R., Ed.) Vol. 2, pp 128−176, Plenum Press, New York
33. Sun, H., Yin, D., and Squier, T. C. (1999) Calcium-dependent structural coupling between opposing globular domains of calmodulin involves the central helix, *Biochemistry 38*, 12266−12279.
34. Lakowicz, J. R., Gryczynski, I., Wiczk, W., Kusba, J., and Johnson, M. L. (1991) Correction for incomplete labeling in the measurement of distance distributions by frequency-domain fluorometry, *Anal. Biochem. 195*, 243−254.
35. Yao, Y., Schoneich, C., and Squier, T. C. (1994) Resolution of structural changes associated with calcium activation of calmodulin using frequency domain fluorescence spectroscopy, *Biochemistry 33*, 7797−7810.
36. Johnson, M. L., and Faunt, L. M. (1992) Parameter estimation by least-squares methods, *Methods Enzymol. 210*, 1−37.
37. Bevington, P. R. (1969) *Data Reduction and Error Analysis for the Physical Sciences*, McGraw-Hill, New York.
38. Lakowicz, J. R., and Gryczynski, I. (1991) Frequency-Domain Fluorescence Spectroscopy, in Topics in Fluorescence Spectroscopy (Lakowicz, J. R., Ed.) Vol. I, pp 293−335, Plenum Press, New York.
39. Beechem, J. M., Gratton, E., Ameloot, M., Knutson, J. R., and Brand, L. (1991) The Global Analysis of Fluorescence Intensity and Anisotropy Decay Data: Second Generation Theory and Programs, in *Topics in Fluorescence Spectroscopy* (Lakowicz, J. R., Ed.) Vol. 2, pp 241−306, Plenum Press, New York.
40. Lamberth, S., Schmid, H., Muenchbach, M., Vorherr, T., Krebs, J., Carafoli, E., and Griesinger, C. (2000) NMR solution structure of phospholamban, *Helv. Chim. Acta 83*, 2141−2152.
41. Chen, Z., Stokes, D. L., Rice, W. J., and Jones, L. R. (2003) Spatial and dynamic interactions between phospholamban and the canine cardiac Ca^{2+} pump revealed with use of heterobifunctional cross-linking agents. *J. Biol. Chem. 278*, 48348−48356.
42. Inesi, G., Zhang, Z., and Lewis, D. (2002) Cooperative setting for long-range linkage of Ca^{2+} binding and ATP synthesis in the Ca^{2+} ATPase, *Biophys. J. 83*, 2327−2332.
43. Zhao, X., Kobayashi, T., Malak, H., Gryczynski, I., Lakowicz, J., Wade, R., and Collins, J. H. (1995) Calcium-induced troponin flexibility revealed by distance distribution measurements between engineered sites, *J. Biol. Chem. 270*, 15507−15514.
44. Sun, H., Yin, D., Coffeen, L. A., Shea, M. A., and Squier, T. C. (2001) Mutation of Tyr^{138} disrupts the structural coupling between the opposing domains in vertebrate calmodulin, *Biochemistry 40*, 9605−9617.
45. Inesi, G., Kurzmack, M., Coan, C., and Lewis, D. E. (1980) Cooperative calcium binding and ATPase activation in sarcoplasmic reticulum vesicles, *J. Biol. Chem. 255*, 3025−3031.
46. Inesi, G. (1987) Sequential mechanism of calcium binding and translocation in sarcoplasmic reticulum adenosine triphosphatase, *J. Biol. Chem. 262*, 16338−16342.
47. Zhang, Z., Lewis, D., Strock, C., Inesi, G., Nakasako, M., Nomura, H., and Toyoshima, C. (2000) Detailed characterization of the cooperative mechanism of Ca^{2+} binding and catalytic activation in the Ca^{2+} transport (SERCA) ATPase, *Biochemistry 39*, 8758−8767.
48. Toyoshima, C., and Nomura, H. (2002) Structural changes in the calcium pump accompanying the dissociation of calcium, *Nature 418*, 605−611.
49. Xu, C., Rice, W. J., He, W., and Stokes, D. L. (2002) A structural model for the catalytic cycle of Ca^{2+}-ATPase, *J. Mol. Biol. 316*, 201−211.
50. Bigelow, D. J., Squier, T. C., and Thomas, D. D. (1986) Temperature dependence of rotational dynamics of protein and lipid in sarcoplasmic reticulum membranes, *Biochemistry 25*, 194−202.
51. Squier, T. C., and Thomas, D. D. (1988) Relationship between protein rotational dynamics and phosphoenzyme decomposition in the sarcoplasmic reticulum Ca-ATPase, *J. Biol. Chem. 263*, 9171−9177.
52. Squier, T. C., Bigelow, D. J., and Thomas, D. D. (1988) Lipid fluidity directly modulates the overall protein rotational mobility of the Ca-ATPase in sarcoplasmic reticulum, *J. Biol. Chem. 263*, 9178−9186.
53. Squier, T. C., Hughes, S. E., and Thomas, D. D. (1988) Rotational dynamics and protein−protein interactions in the Ca-ATPase mechanism, *J. Biol. Chem. 263*, 9162−9170.
54. Hunter, G. W., Bigelow, D. J., and Squier, T. C. (1999) Lysophosphatidylcholine modulates catalytically important motions of the Ca-ATPase phosphorylation domain, *Biochemistry 38*, 4604−4612.
55. Hunter, G. W., Negash, S., and Squier, T. C. (1999) Phosphatidylethanolamine modulates Ca-ATPase function and dynamics, *Biochemistry 38*, 1356−1364.
56. Levine, B. A., Patchell, V. B., Sharma, P., Gao, Y., Bigelow, D. J., Yao, Q., Goh, S., Colyer, J., Drago, G. A., and Perry, S. V. (1999) Sites on the cytoplasmic region of phospholamban involved in interaction with the Ca2+-activated ATPase of the sarcoplasmic reticulum. *Eur. J. Biochem. 264*, 905−913.
57. Voss, J., Jones, L. R., and Thomas, D. D. (1994) The physical mechanism of calcium pump regulation in the heart. *Biophys. J. 67*, 190−196.
58. Stokes, D. L., and Green, N. M. (2003) Structure an function of the calcium pump. *Annu. Rev. Biophys. Biomol. Struct. 32*, 445−468.
59. Toyoshima, C., Nakasako, M., Nomura, H., and Ogawa, H. (2000) Crystal structure of the Ca^{2+} pump of sarcoplasmic reticulum at 2.6 Å resolution. *Nature 405*, 647−655.
60. Hutter, M. C., Krebs, J., Meiler, J., Griesinger, C., Carafoli, E., and Helms, V. (2002) A structural model of the complex formed by phospholamban and the calcium pump of sarcoplasmic reticulum obtained by molecular mechanics. *Chembiochem. 3*, 1200−1208.
61. Coll, K. E., Johnson, R. G., Jr., and McKenna, E. (1999) Relationship between phosholamban and nucleotide activation of cardiac sarcoplasmic reticulum Ca2+ adenosinetriphosphatase. *Biochemistry 38*, 2444−2451.
62. Huang, S., Negash, S., and Squier, T. C. (1998) Erythrosin isothiocyanate selectively labels lysine464 within an ATP-protectable binding site on the Ca-ATPase in skeletal sarcoplasmic reticulum membranes. *Biochemistry 37*, 6949−6957.
63. Toyofuku, T., Kurzydlowski, K., Tada, M., and MacLennan, D. H. (1994) Amino acids Lys-Asp-Asp-Lys-Pro-Val402 in the Ca-(2+)-ATPase of cardiac sarcoplasmic reticulum are critical for functional association with phospholamban, *J. Biol. Chem. 269*, 22929−22932.
64. Fairclough, R. H., and Cantor, C. R. (1978) The use of singlet−singlet energy transfer to study macromolecular assemblies, *Methods Enzymol. 48*, 347−379.
65. Stryer, L. (1978) Fluorescence energy transfer as a spectroscopic ruler, *Annu. Rev. Biochem. 47*, 819−846.

BI036183U